Design of composite lattice materials combined with fabrication approaches

Jun Xu[1, 2, 3, 4], Yaobo Wu[1, 2], Xiang Gao[1, 2], Huaping Wu[5], Steven Nutt[6], Sha Yin[1, 2, 3*]

[1]*Department of Automotive Engineering, School of Transportation Science and Engineering, Beihang University, Beijing, China, 100191*

[2]*Advanced Vehicle Research Center (AVRC), Beihang University, Beijing, China, 100191*

[3]*State Key Laboratory for Strength and Vibration of Mechanical Structures, School of Aerospace Engineering, Xi'an Jiaotong University, Xi'an, China, 710049*

[4]*State Key Laboratory for Automotive Safety and Energy, Tsinghua University, Beijing, China, 100084*

[5]*Key Laboratory of E&M (Zhejiang University of Technology), Ministry of Education & Zhejiang Province, Hangzhou 310014, PR China*

[6]*Department of Chemical Engineering and Materials Science, University of Southern California, Los Angeles, CA 90089-0241, USA*

Abstract: Lattice materials can be designed through their microstructure while concurrently considering fabrication feasibility. Here, we propose two types of composite lattice materials with enhanced resistance to buckling: (a) hollow lattice materials fabricated by a newly-developed bottom-up assembly technique and the previously developed thermal expansion molding technique; (b) hierarchical lattice materials with foam-core sandwich trusses fabricated by interlocking assembly process. The mechanical performance of sandwich structures featuring the two types of lattice cores were tested and analyzed theoretically. For hollow lattice core material, samples from two different fabrication processes were compared and both failed by nodal rupture

* Corresponding author: Prof. Sha Yin, E-mail: shayin@buaa.edu.cn. Tel: +86-10-82339921, Fax: +86-10-82339923

or debonding. In contrast, hierarchical lattice structures failed by shear buckling without interfacial failure in the sandwich struts. Calculations using established analytical models indicated that the shear strength of hollow lattice cores could be optimized by judicious selection of the thickness of patterned plates. Likewise, the shear strength of hierarchical foam-core truss cores could be maximized (with minimal weight) through design of truss geometry. The bottom-up assembly technique could provide a feasible way for mass-production of lattice cores, but the design about how to assembly is critical. Hierarchical lattice cores with foam sandwich trusses should be a relatively ideal choice for future lightweight material application.

Keywords: Sandwich structure; Lattice materials; Fiber composites; Mechanical properties; Structural design; Mass production.

1. INTRODUCTION

Lattice materials are regarded as viable lightweight and multifunctional candidates for the next generation of efficient structures due to their superior specific strength and stiffness [1-3], large interconnected open space [4-5], and energy absorption capability [6-8]. Selection of fiber composites as constituent materials for lattice cores can lead to specific mechanical properties that surpass those of metallic counterparts in engineered systems [9]. Various reports have documented efforts over the past decade to explore fiber reinforced lattice composites [10-15], and these efforts encompass techniques for producing lattice core structures, such as hot press molding, weaving [16, 17], interlocking [18] and additive assembly manufacturing [19].

Microstructural design of lattice materials can be an effective pathway to increase buckling resistance and thus specific properties while achieving ultra-low relative density. In particular, design of truss cross-section has been proven to be an effective strategy. For example, pyramidal

lattice materials with hollow trusses exhibit greater plastic buckling strength than solid truss counterparts [5, 20-22]. The use of hollow trusses increases the resistance to elastic or plastic buckling because of the greater second moments of inertia compared to solid trusses. Moreover, the space inside the hollow trusses can be filled with a second functional phase to impart additional functionality [23]. Hwang et al developed a semi-circular pyramidal kagome sandwich structure and studied their bending performance [24]. By employing a hierarchical strategy, stretch-stretch hybrid lattice cores with self-similar lattice sandwich trusses and stretch-bend hybrid lattice cores with foam sandwich trusses were demonstrated to be as efficient as hollow lattice cores after optimization [25-26]. On the other hand, the outstanding mechanical performance of sandwich structures with enhanced lattice cores must be guranteed by perfect facesheet-core interface, and thus the shear performace of those enhanced lattice cores should not be neglected.

Materials design ideally should also encompass manufacturing and cost factors, both of which are critical for engineering application. To illustrate this need, consider the work of Yin et.al, who demonstrated developed a thermal expansion molding approach to fabricate hollow pyramidal lattice comprised of composite materials that yielded superior mechanical properties compared with solid analogs of similar low density [22]. However, the process was relatively complex, and was not sufficiently robust to be compatible with large-scale production of automotive parts. In contrast, hierarchical lattice cores with foam sandwich trusses were fabricated using hot-press molding combined with an interlocking assembly method, which was relatively easier, and facesheet wrinkling in the foam sandwich strut occurred readily during compression, which was attributed to the poor interfacial adhesion between foam and facesheets [26].

Lattice materials produced by mass-production approaches is a largely underdeveloped domain in the technology of core materials, despite the critical role it plays in adaptation. Thus, the objective of this work is to seek simpler methods for large-volume production of two types of composite lattice cores cited above, and then evaluate the process by structural overall performance. First, we describe a flexible bottom-up assembly method for hollow lattice cores. This mold-free technique shares the same processing idea as the micro/nano additive manufacturing method. In addition, we describe a vacuum bag only process combined with interlocking assembly method for producing foam-core hierarchical lattice cores, so as to increase the interfacial properties of foam sandwich trusses. The mechanical performance of the two types of structures is discussed and analyzed. Finally, theoretical models are employed for prediction of properties and further optimization, which provides a means to evaluate the fabrication approach as well.

2. EXPERIMENTAL

2.1. Fabrication of composite lattice core sandwich structures with hollow trusses

A flexible and mold-free, bottom-up assembly method is proposed to fabricate hollow composite lattice cores besides the previously developed thermal expansion molding method. For the bottom-up fabrication technique, trusses and perforated sheets were used for positioning as basic elements. Unidirectional pultruded composite rods (solid and hollow) were used for truss elements. Pre-drilled laminates were used to situate trusses and guide truss insertion. The perforated guide plates featured custom designed patterns, as shown in Figures 1a-b. Two-dimensional perforated guide plates with inclined holes were produced, and the representative unit cell of this intermediate layer (between facesheets and lattice core) is shown schematically in

Figure 1c. A patterned composite plate made from woven fiber-glass is shown in Figure 1d. The relative density of the patterned plate after perforation can be expressed as

$$\bar{\rho}_{\text{int}} = \frac{m^2 - 2n^2 - \pi d_o^2 / \sin\omega}{m^2} \qquad (1)$$

where $m = \left(\sqrt{2}l_1 \cos\omega + 2l_2\right)$ is related to the geometry of the pyramidal lattice structure; n is the edge dimension of the square hole in the perforated sheet, and ω=45° is the inclination angle. Note that due to the limitations of laboratory processing conditions in this study, elliptical through-thickness holes of diameter d_0 were drilled in the lattice sheets by projection of inclined tubes.

An illustration showing the insertion of trusses is shown in Figure 2a. Before insertion, hollow trusses were cut to specific lengths with ends at angle ω according to the final truss configuration. During the process, we first inserted trusses into four corners, then into arrays along lattice sheet edges, and finally the middle array of holes. Figure 2b shows the assembled hollow lattice core, and the 2-D planar lattice sheet functioning as attachment to the hollow lattice core. In the following section, we describe how the core assemblies were co-bonded with two carbon fiber composite facesheets (3234/T700, Beijing Institute of Aeronautical Materials, China) using epoxy film adhesive to form the hollow lattice core sandwich structures in Figure 2c.

The 2-D lattice sheets can be considered as intermediate layers connecting the facesheets and the hollow lattice cores. A schematic of the representative unit cell, including patterned plate, is shown in Figure 2d, and defines the relevant geometric parameters of the lattice structure. The relative density $\bar{\rho}$ is given by the ratio of the solid volume to that of the unit cell:

$$\bar{\rho} = \frac{V_s}{V^*} = \frac{2t_{\text{int}}(m^2 - 2n^2 - \pi d_o^2 / \sin\omega) + l_1\pi(d_o^2 - d_i^2)}{m^2 h} \quad (2)$$

where l_1 is the truss length, and l_2 represents the side of the square at the top of a pyramidal core; d_o and d_i are the outer and inner diameters of the hollow trusses; $h = l_1 \sin\omega$ is the height of the unit cell, and t_{int} is the thickness of the patterned plate. In the present study, l_1=19.8 mm, l_2=15 mm, t_{int}=2 mm, and the relative densities of the patterned plate and the pyramidal cores are summarized in Table 1.

2.2. Fabrication of composite lattice core sandwich structures with foam sandwich trusses

(1) Vacuum Bag Only (VBO) process for foam sandwich panels

Foam core composite panels were fabricated for the following assembly of lattice truss cores. Glass fiber epoxy prepreg with plain weave reinforcement was selected and specifically formulated for sandwich panel fabrication (3238A/EW250F, Beijing Institute of Aeronautical Materials, China). PMI foam (Rohacell-55 WF-HT). The material was chosen because of its lightweight and the capacity to sustain processing pressure at high temperature. The mechanical properties of foam and glass fiber prepreg together with carbon fiber prepreg are summarized in Table 2.

Vacuum Bag Only (VBO) processing was used to produce glass fiber foam sandwich panels. The details of the composite layup schemes are presented in Figure 3a. The layup in the sandwich panel is symmetric about the mid-plane, and two prepreg layers were laid up followed with a piece of foam and another two prepreg layers. After layup, samples were vacuum bagged (>

0.09 MPa), and bagged samples were debulked for 1h at room temperature to remove trapped air. After the room-temperature vacuum hold, samples were cured according to the recommended cure cycle (Figure 3b), then cooled to room temperature.

(2) Interlocking assembly method for the hierarchical composite lattice cores

Laminated sandwich panels were cut into strips and then grooved to produce the geometries indicated above. Strips were subsequently joined by slot insertion at the nodes to form the lattice cores, and the nodes were secured with epoxy adhesive as introduced in a former publication [26]. The lattice cores with foam sandwich struts were bonded with two laminates, forming the corresponding sandwich structures, as shown in Figure 3c, for subsequent testing. The effective density of the representative unit cell shown in Figure 3d is deduced as

$$\rho_{\text{eff}} = \frac{2b\left[l_1 + l_2 - b\tan\frac{\omega}{2}\right]\left(2t_f\rho_f + t_c\rho_c\right)}{\left[l_1\cos\omega + l_2 - b\tan\frac{\omega}{2}\right]^2\left(l_1\sin\omega + b\right)} \qquad (3)$$

where l_1 and b are length and width of the sandwich strut; l_2 is the length of the horizontal trusses which connects the inclined struts at the pyramidal node and ω is the inclination angle between the struts and the base of the unit cell. The thickness and density of the foam core in the sandwich strut is t_c and ρ_c, while the facesheet thickness and density is t_f and ρ_f. Here, l_1= 16.97 mm, l_2 = 12 mm, b = 3 mm, t_f = 0.4 mm, t_c = 4 mm, ρ_c = 0.052 g/cm^3, ρ_f = 1.8 g/cm^3. Thus, the effective density of the hierarchical core is 0.0353 g/cm^3.

2.3. Mechanical testing method

For hollow lattice cores, the compressive properties can be referred to Ref. [22], and only shear tests were performed here. For compression tests, hierarchical lattice cores with 3*3 cells were prepared, and through-thickness tests were performed following the guidelines of ASTM C365/C365M as shown in Figure 4a. For shear tests, samples with 2*4 unit cells were prepared in accordance with ASTM C273/C273M-06. Composite lattice core sandwich structures with hollow trusses and foam sandwich trusses were both tested on a hydraulic servo testing machine (MTS 810) with a 100 kN load cell using a single-lap shear configuration in Figure 4b at an applied nominal shear strain rate of 1 mm/min. The measured load cell force was used to calculate the shear stress while the relative sliding of the two faces of sandwich plates was measured using a laser extensometer. The shear strain was calculated from the sliding displacement.

3. THEORETICAL ANALYSIS

3.1. Effective shear properties of composite lattice cores with hollow trusses

Analysis of the effective shear properties of hollow truss composite pyramidal lattice structure was undertaken by considering the deformation of a single tube from a unit cell, as sketched in Figure 5. Note that trusses produced by the bottom-up technique are constrained by both the facesheets and the intermediate layers (if perfectly bonded), and thus the boundary constraint coefficients k are assumed to be $k = 2$ for the two techniques described above.

3.1.1. Shear stiffness

An imposed in-plane displacement δ_x in the x-direction gives rise to a shear angle γ_{xz} and a resultant force F_{xz}. Two truss members will be loaded in compression, while the other two will be

loaded in tension. Assuming that the tensile modulus equals to the compressive modulus E_c of composite tubes, the shear stiffness can be given as

$$G = E_c \bar{\rho}_h \sin^2 \omega \left[\cos^2 \omega + \frac{3}{4} \frac{d_o^2 + d_i^2}{l_1^2} \sin^2 \omega \right] \qquad (4)$$

which is independent of loading direction ψ （ψ=45^0）. The first and second terms in Eq. (4) represent the tube stretching and bending contributions, respectively.

3.1.2. Shear strength

The transverse shear strength τ depends on the loading direction ψ ($\psi = \pi/4$) in the present study. Four competing failure modes are possible for hollow trusses: tensile fracture, compressive fracture, Euler buckling, and node failure (rupture or debonding). However, the tensile fracture strength is generally greater than the compressive fracture strength for composites, and thus tensile fracture is unlikely to occur. Moreover, considering the competition between Euler buckling and fracture of composite tubes based on the compressive properties given in Ref. [22], fracture will always be the governing failure mode of trusses with the tube dimensions in the present study. Accordingly, truss fracture and node failure will be the only two practical failure modes that determine the shear strength, and we will derive the corresponding analytical shear strength for each.

If trusses fail by compressive fracture at a stress of σ_{cf}, the transverse shear strength of a lattice core with hollow trusses can be predicted by

$$\tau(\psi) = \frac{\sigma_{cf} \bar{\rho}_h \sin \omega}{\cos \psi} \left(\cos \omega + \frac{3}{4} \frac{d_o^2 + d_i^2}{l_1^2} \frac{\sin^2 \omega}{\cos \omega} \right) \qquad (5)$$

If trusses fail by node rupture, shear failure mechanisms are different for structures produced by the two techniques.

(1) Samples produced by thermal expansion molding.

The progressive failure process starts at the node ends where the truss fibers are twisted and embedded into the face sheet. The transverse shear strength of a lattice core with hollow trusses can be derived as

$$\tau = \frac{2F_{nr}}{(l_1 \cos\omega + \sqrt{2} l_2)^2} \qquad (6)$$

where F_{nr} is the peak load of a sandwich plate with a single inclined truss (produced by the same fabrication process) in transverse shear loading. Note that the value of F_{nr} is correlated only to the fabrication details at the truss ends.

(2) Samples produced by bottom-up assembly

Truss pullout occurs readily at truss-sheet junctions as shown in Figure 6b. The interface between lattice trusses and facesheet is identified as Interface 1, while the interface between lattice trusses and intermediate layers will be called Interface 2. Truss peel-off occurs only when the shear force triggers debonding at both Interface 1 and Interface 2, and thus the shear forces from Interface 1 and 2 will contribute to the shear strength of the entire structure. Thus, the shear strength of lattice structures is expressed as

$$\tau = \tau_n \overline{\rho_h} + 4 \frac{\tau_n d_o \overline{\rho_h} \cos\omega}{(d_o^2 - d_i^2)} t_{\text{int}} \qquad (7)$$

where τ_n is the adhesive shear strength between the plate and the trusses, and t_{int} is the thickness of the patterned plates. The first term in Eq.7 bodies the adhesive shear force in Interface 1, while the second item expresses the shear force in Interface 2. However, due to the limits of the laboratory fabrication methods for producing the holes in this study, only the adhesive shear force in Interface 1 contributes to the overall shear strength.

3.2. Effective shear properties of composite lattice cores with foam sandwich trusses

Theoretical deduction about the out-of-plane compressive properties for hierarchical lattice cores can be referred to Ref. [26], and the shear performance can be analyzed in a similar way.

3.2.1. Shear stiffness

The shear stiffness of the hierarchical lattice cores with foam sandwich trusses can be given by

$$G = \frac{(l_1 \sin\omega + b)}{\left[l_1 \cos\omega + l_2 - b\tan\frac{\omega}{2}\right]^2}\left[\frac{\cos^2\omega}{\frac{l_1}{A_{sand}}} + \frac{\sin^2\omega}{\frac{l_1^3}{12D_{sand}} + \frac{l_1}{A_{sand}}}\right] \qquad (8)$$

where $A_{sand} = 2E_f^{eq} b t_f$ is compressive stiffness of the foam core sandwich strut, $S_{sand} = G_c b t_c$ is shear stiffness, and $D_{sand}^{I} = \frac{1}{6} E_f^{eq} t_f b^3$ is the bending stiffness. For the selected foam (Rohacell 55WF-HT) in this paper, the measured density $\rho_c = 52k\text{g/m}^3$, Young's modulus $E_c = 75\text{MPa}$, shear modulus $G_c = 28.125\text{MPa}$, and shear strength $\tau_c = 0.8\text{MPa}$.

3.2.2 Shear strength

When hierarchical lattice truss sandwich structures bear shear load, several competing failure modes are possible to occur, i.e., tensile failure, nodal failure, debonding, facesheet crushing (plastic microbuckling) or wrinkling of foam sandwich struts, shear failure of foam core, Euler or shear buckling of sandwich struts. The last five failure modes occur only in compressive struts, and the tensile strength of the struts is generally greater than the compressive strength. Also, debonding failure between the facesheet and lattice truss cores can occur under shear loading. Thus, the transverse shear strength τ for different failure modes was derived, described below.

(a) Facesheet plastic microbuckling of foam sandwich struts

Compressive load may trigger plastic microbuckling of facesheets in sandwich struts when the compressive stress reaches the plastic microbucking strength of composite facesheet σ_f which is measured by independent experiment. The corresponding shear strength is given as

$$\tau = \frac{2\sigma_f b t_f \cos\omega}{\cos\varphi\left[l_1\cos\omega + l_2 - b\tan\frac{\omega}{2}\right]^2}\left[1 + \frac{\sin^2\omega}{\cos^2\omega A_{sand}\left(\frac{l_1^2}{12D_{sand}} + \frac{1}{S_{sand}}\right)}\right] \quad (9)$$

(b) Facesheet wrinkling of sandwich struts

Compressive load may result in face-sheet wrinkling of sandwich struts. The compressive force can be expressed as $F_a = \left(E_f E_c G_c\right)^{1/3} b t_f$, and thus the shear strength of lattice sandwich core is

$$\tau = \frac{\left(E_f E_c G_c\right)^{\frac{1}{3}} b t_f \cos\omega}{\cos\varphi\left[l_1\cos\omega + l_2 - b\tan\frac{\omega}{2}\right]^2}\left[1 + \frac{\sin^2\omega}{\cos^2\omega A_{sand}\left(\frac{l_1^2}{12D_{sand}} + \frac{1}{S_{sand}}\right)}\right] \quad (10)$$

(c) Shear failure of foam core

Shear force applied on a strut will induce shear failure of the foam core. The maximum shear force in the foam strut is $F_s = \tau_c t_c b$, τ_c is the foam shear strength. Then, the shear strength of the lattice sandwich cores is

$$\tau = \frac{\tau_c t_c b \sin\omega}{\cos\varphi\left[l_1\cos\omega + l_2 - b\tan\frac{\omega}{2}\right]^2}\left[1 + \frac{\cos^2\omega A_{sand}\left(\frac{l_1^2}{12D_{sand}} + \frac{1}{S_{sand}}\right)}{\sin^2\omega}\right] \quad (11)$$

(d) Euler buckling of sandwich struts

Struts are likely buckle when compressed. The Euler buckling load of foam sandwich struts with a fixed boundary condition is $F_a = 4\pi^2 D_{sand} / l_1^2$, and the shear strength is given by

$$\tau = \frac{4\pi^2 D_{sand}\cos\omega}{l_1^2\cos\varphi\left[l_1\cos\omega + l_2 - b\tan\frac{\omega}{2}\right]^2}\left[1 + \frac{\sin^2\omega}{\cos^2\omega A_{sand}\left(\frac{l_1^2}{12D_{sand}} + \frac{1}{S_{sand}}\right)}\right] \quad (12)$$

(e) Shear buckling of sandwich struts

Shear buckling will possibly occur when compressive force reaches the critical load at $F_a = G_c t_c b$. The shear strength can be expressed as

$$\tau = \frac{G_c t_c b \cos\omega}{\cos\varphi\left[l_1\cos\omega + l_2 - b\tan\frac{\omega}{2}\right]^2}\left[1 + \frac{\sin^2\omega}{\cos^2\omega A_{sand}\left(\frac{l_1^2}{12D_{sand}} + \frac{1}{S_{sand}}\right)}\right] \quad (13)$$

(f) Debonding

Debonding can occur when the shear strength at the facesheet-lattice core interface is exceeded. The shear strength is related to the bond area as

$$\tau = \tau_n \frac{2l_2 b - b^2}{2\left[l_1\cos\omega + l_2 - b\tan\frac{\omega}{2}\right]^2} \quad (14)$$

3.3. Optimal design

3.3.1. Composite lattice cores with hollow trusses

Based on the analysis described above, we can design nodal properties (and thus shear performance) using the bottom-up assembly technique for a specific truss configuration by selection of an appropriate patterned plate (e.g., length *n*, thickness t_{int}). Analytical models showed that nodal or interfacial strength can be increased by increasing the thickness of the patterned plates. When the thickness is increased to a specific value, we assume that the shear force contributed by adhesive shear from Interfaces 1 and 2 is equal to the truss failure force. Optimal design involves competition between truss failure and nodal debonding, and thus the shear strength

will be maximized with the optimal thickness that provides the greatest shear strength values at minimal weight introduced by the patterned sheet.

$$t_{\text{int}}^{optimal} = \left(\frac{\sigma_{cf} \sin 2\omega}{2\cos\psi} - \tau_n \right) \frac{\left(d_o^2 - d_i^2\right)}{4\tau_n d_o \cos\omega} \qquad (15)$$

where σ_{cf} = 188 MPa is truss failure stress, τ_n = 20 MPa is shear strength of adhesive. The optimal thickness, which is related to the cross-sectional area of hollow trusses, is shown in Table 3 for different truss geometries. From the results, the corresponding optical thickness of the patterned plate increases as the inner diameter decreases. Accordingly, hollow trusses with thinner wall thickness (larger d_i), which require thinner patterned sheets, must be selected for practical applications, and thus the weight penalty of the patterned sheet will be minimal. From Eq. 15 material properties, including density, will not affect the optimal thickness, and thus other common cellular materials (such as polymer or metallic foams) with lower density, may provide attractive options for the patterned sheets in this study, provided the panels themselves do not fail before the adhesive.

3.3.2. Composite lattice cores with foam sandwich trusses

The optimal geometries of the hierarchical lattice cores (*e.g.* t_f, l_2) can be determined for the maximum shear strength with the minimum weight. From the predictive models, the optimal facesheet thickness t_f of sandwich strut and the optimal length l_2 of the horizontal trusses can be deduced with given property and geometries of foams as follows.

$$t_f = \frac{G_c t_c}{2\sigma_f} \qquad (16)$$

and

$$l_2 = t_c \frac{G_c}{\tau_n} \frac{\cos\omega}{\cos\varphi} + \frac{b}{2} \qquad (17)$$

4. RESULTS AND DISCUSSION

4.1. Composite lattice cores with hollow trusses

The shear stress-strain curves and the representative failure modes of three hollow lattice core sandwich structures with different relative densities fabricated by the bottom-up assembly technique are shown in Figure 6. The stress increases linearly before reaching the peak, associated with node debonding at the truss and interlayer interface, followed by stress fluctuations and a sharp drop, which corresponds to node failure at truss ends. The shear strength for the three structures increases with core density, but the corresponding failure mode (tube-facesheet debonding) remains the same, as shown in Figure 6b.

Figure 7 shows the shear behavior of sandwich structures with similar truss geometries produced using thermal expansion molding. The curves in Figure 7a differ from those in Figure 6a, exhibiting nonlinear behavior prior to the peak stress, followed by a gradual decline in (fluctuating) stress associated with progressive node rupture. For structures with relative density of 1.07%, trusses in compression failed by crushing, while trusses in tension failed by node rupture. However, lattice structures with relative density of 2.21% and 4.53% both failed exclusively by node rupture.

4.2. Composite lattice cores with foam sandwich trusses

The measured compressive stress-strain curves are plotted in Figure 8a along with theoretical prediction. The nominal compressive stress increases almost linearly with the nominal strain and reaches a peak. Shear buckling of sandwich lattice struts happened at the peak stress with a failure strain of 0.026 following with a sharp stress drop. The measured shear stress-strain curve of the hierarchical lattice cores with foam sandwich trusses is plotted in Figure 8b. After an initial increase, the shear stress reaches a peak, followed by a sharp drop and a long stress plateau. The governing failure mode observed in the shear tests is also shear buckling of sandwich struts.

The measured compressive strength differs from predicted value by 11%. Also, the shear strength value obtained from the theoretical models is included in Figure 8b. The deviation between measured shear strength and predicted shear strength can be attributed to sample misalignment, and the adhesive layer may introduce relative displacement of the loading plates. The measured shear strength differs from predicted values by 14%. The difference can be attributed to fabrication defects and actual geometries departing from ideal ones (t_c in the obtained sandwich strut is about 3 mm here).

4.3. Comparison

A comparison between analytical predictions and experimental results is summarized in Table 4 for hollow lattice cores fabricated by thermal expansion molding (Variant 1), bottom-up assembly (Variant 2) and for hierarchical lattice cores with foam sandwich trusses (Variant 3). From the analytical results in Table 4, for hollow lattice cores, we can assume that when hole of the patterned plate and rod are assembled (snug) and the adhesion area is sufficiently large, the corresponding shear strength could be guaranteed. Thus, the bottom-up assembly technique

provides one way for the mass-production of hollow lattice cores, but the design about the assembly and especially the joints could be improved.

The structural efficiency of the two structures can be compared. As indicated in a previous publication for compressive properties [26], hierarchical lattice cores with foam sandwich struts, after optimization, can be as efficient as hollow lattice cores. Considering fabrication reliability, the two types of structures may be well-suited to engineering applications because of the high specific strength and stiffness and intrinsic resistance to buckling.

5. CONCLUSIONS

Enhanced lattice materials derived from cross-sectional design of lattice trusses and produced using different fabrication approaches were examined. A bottom-up assembly technique was described for mass production of hollow lattice core sandwich structures using commercial composite elements (plates, tubes or rods) and perforated patterned plates for subsequent tube insertion. For hierarchical lattice cores with foam sandwich trusses, a vacuum bag only process combined with interlocking assembly method was developed using glass fiber prepreg and PMI foam. The mechanical performance of the two types of structures were tested and predicted theoretically. For hollow lattice cores, the shear strength of samples produced by thermal expansion molding was greater than those produced by bottom-up assembly method, but both node rupture or debonding were observed. However, simple analytical models indicated that if the nodal or interfacial strength is sufficiently strong, the structures can provide superior shear strength, and one can determine the optimal thickness of the patterned panels to maximize the interfacial shear strength with minimal weight penalty. For hierarchical lattice materials, shear buckling was observed during compression and shear tests, and no interfacial failure in the sandwich struts

occurred. The mechanical models accurately predict the shear properties of the enhanced lattice materials, and optimized truss geometries of foam sandwich struts are deduced.

The bottom-up assembly technique provides a feasible way for mass-production of hollow lattice cores, but the design about how to assembly could be improved in future work. Also, alternative cellular materials, such as foams, with strength exceeding shear strength of adhesives, may provide additional choices for patterned plates in hollow lattice cores. The structural efficiency of the two types of lattice cores considered in the present study is the same after optimization. Combined with fabrication process, hierarchical lattice cores with foam sandwich trusses should be a better choice to future lightweight material application.

Acknowledgements: This work is financially supported by the National Natural Science Foundation of China under grant No. 11402012, Young Elite Scientist Sponsorship Program by CAST, Opening fund of State Key Laboratory for Strength and Vibration of Mechanical Structures, Xi'an Jiaotong University (SV2015-KF-07, SV2016-KF-20), Opening fund of State Key Laboratory for Automotive Safety and Energy, Tsinghua University (Grant No. KF16142), and Beijing Municipal Science & Technology Commission (Grant No.Z161100001416006).

References:

1. Dong L, Wadley H. Shear response of carbon fiber composite octet-truss lattice structures. *Compos Part A-Appl S* 2016; 81: 182-192.
2. Evans AG, Hutchinson JW, Fleck NA, et al. The topological design of multifunctional cellular metals. *Prog Mater Sci* 2001; 46: 309-327.
3. Xu J, Zhang W, Gao X, Meng W, et al. Strain Rate and Anisotropic Microstructure Dependent Mechanical Behaviors of Silkworm Cocoon Shells. *PLoS One* 2016, 11(3): e0149931.
4. Biagi R, Bart-Smith H. Imperfection sensitivity of pyramidal core sandwich structures. *Int J Solids Struct* 2007; 44: 4690-4706.
5. Rathbun HJ, Zok FW, Waltner SA, et al. Structural performance of metallic sandwich beams with hollow truss cores. *Acta Mater* 2006; 54: 5509-5518.
6. Queheillalt DT, Wadley HNG. Cellular metal lattices with hollow trusses. *Acta Mater* 2005;

53: 303-313.
7. Kooistra GW, Queheillalt DT and Wadley HNG. Shear behavior of aluminum lattice truss sandwich panel structures. *Mat Sci Eng a-Struct* 2008; 472: 242-250.
8. Yungwirth CJ, Radford DD, Aronson M, et al. Experiment assessment of the ballistic response of composite pyramidal lattice truss structures. *Compos Part B-Eng* 2008; 39: 556-569.
9. Margossian A, Bel S and Hinterhoelzl R. Bending characterization of a molten unidirectional carbon fibre reinforced thermoplastic composite using a Dynamic Mechanical Analysis system. *Compos Part A-Appl S* 2015; 77: 154-163.
10. Wang B, Zhang G, He Q, et al. Mechanical behavior of carbon fiber reinforced polymer composite sandwich panels with 2-D lattice truss cores. *Mater Design* 2014; 55: 591-596.
11. Li XD, Wu LZ, Ma L, et al. Fabrication and mechanical properties of composite pyramidal truss core sandwich panels with novel reinforced frames. *J Reinf Plast Comp* 2016; 35(16): 1260-1274.
12. Wang SX, Wu LZ and Ma L. Low-velocity impact and residual tensile strength analysis to carbon fiber composite laminates. *Mater Design* 2010; 31: 118-125.
13. Lou J, Ma L and Wu LZ. Free vibration analysis of simply supported sandwich beams with lattice truss core. *Mater Sci Eng B-Adv* 2012; 177: 1712-1716.
14. Yin S, Li J, Liu B, et al. Honeytubes: Hollow lattice truss reinforced honeycombs for crushing protection. *Compos Struct*, 2016; 160: 1147-1154.
15. Wang P, Sun F, Fan H, et al. Retrofitting scheme and experimental research of severally damaged carbon fiber reinforced lattice-core sandwich cylinder. *Aerosp Sci Technol* 2016; 50: 55-61.
16. Kazemahvazi S, Khokar N, Hallstrom S, et al. Confluent 3D-assembly of fibrous structures. *Compos Sci Technol* 2016; 127: 95-105.
17. Song ZZ, Cheng S, Zeng T, et al. Compressive behavior of C/SiC composite sandwich structure with stitched lattice core. *Compos Part B-Eng* 2015; 69: 243-248.
18. Finnegan K, Kooistra G, Wadley HNG, et al. The compressive response of carbon fiber composite pyramidal truss sandwich cores. *Int J Mater Res* 2007; 98: 1264-1272.
19. Cheung KC, Gershenfeld N. Reversibly Assembled Cellular Composite Materials. *Science* 2013; 341: 1219-1221.
20. Evans A G, He M Y, Deshpande V S, et al. Concepts for enhanced energy absorption using hollow micro-lattices. *Int J Impact Eng*, 2010; 37(9): 947-959.
21. Queheillalt DT, Wadley HNG. Pyramidal lattice truss structures with hollow trusses. *Mat Sci Eng a-Struct* 2005; 397: 132-137.
22. Yin S, Wu L, Ma L, et al. Pyramidal lattice sandwich structures with hollow composite trusses. *Compos Struct*, 2011; 93(12): 3104-3111.
23. Yin S, Wu L, Ma L, Nutt S. Hybrid truss concepts for carbon fiber composite pyramidal lattice structures. *Compos Part B-Eng* 2012; 43: 1749-1755.
24. Hwang J S, Choi T G, Lyu M Y, et al. Investigation for the bending modes of a semi-circular pyramidal kagome sandwich structure and the bending load calculation. *Compos Struct,* 2015; 134: 10-17.
25. Yin S, Wu L, Nutt S R. Compressive efficiency of stretch–stretch-hybrid hierarchical composite lattice cores. *Materials & Design*, 2014; 56(4): 731-739.
26. Yin S, Wu L, Ma L, Nutt S. Pyramidal lattice sandwich structures with hollow composite trusses. *Compos Struct* 2011; 93: 3104-3111.

Table 1. Relative densities of the patterned sheet before and after perforation, and those of hollow pyramidal cores neglecting the patterned sheet ($\overline{\rho}_h$, before assembly) and including the patterned sheet ($\overline{\rho}$, after assembly).

Materials	Shape	d_o (mm)	d_i (mm)	Relative density before perforation/assembly	Relative density after perforation/assembly
Patterned sheet	2-D lattice	6	-	46%	40%
Hollow pyramidal core	3-D lattice	6	5.4	1.07%	12.69%
		6	4.5	2.21%	14.29%
		6	3	4.53%	16.29%

Table 2. Mechanical properties of raw materials

Properties	Materials		
	Glass fiber prepreg	Carbon fiber prepreg	PMI foam
Tensile modulus (GPa)	25	69	75
Tensile strength (MPa)	380	756	1.6
Compressive modulus (GPa)	25	64	75
Compressive strength (MPa)	380	557	0.8
In-plane shear modulus (GPa)	4.5	4.2	24
In-plane shear strength (MPa)	80	118	0.8
Bending modulus (GPa)	21	59	-
Bending strength (MPa)	450	924	-
Interlayer shear strength (MPa)	45	68	

Table 3. The optimal geometries of the enhanced lattices core for the maximum shear properties with the minimum weight.

Composite lattice cores with hollow trusses			
Materials of patterned sheet	d_o **(mm)**	d_i **(mm)**	**Optimal thickness (mm)**
Carbon fiber composites	6	5.4	2.3
	6	4.5	5.3
	6	3	9.0
Composite lattice cores with foam sandwich trusses			
Materials of sandwich core	t_f **(mm)**		l_2 **(mm)**
PMI 51 WF	0.15		7.12

Table 4. Comparison between experimental data and theoretical prediction for hollow lattice cores fabricated by the thermal expansion molding approach (Variant 1), bottom-up assembly technique (Variant 2) and hierarchical lattice cores with foam sandwich trusses (Variant 3).

Composite lattice cores with hollow trusses			
Samples	**Relative density** $\overline{\rho}_h$	**Predicted strength (MPa)**	**Measured Strength (MPa)**
Variant 1a	1.07%	0.46	0.48
Variant 1b	2.21%	0.97	0.89
Variant 1c	4.53%	0.97	0.91
Variant 2a	1.07%	$\frac{1.27}{0.22}$ (the first item in Eq.7)	0.2
Variant 2b	2.21%	$\frac{1.39}{0.44}$ (the first item in Eq.7)	0.32
Variant 2c	4.53%	$\frac{2.04}{0.91}$ (the first item in Eq.7)	0.71
Composite lattice cores with foam sandwich trusses			
Variant 3	8.14%	0.69 (compression) 0.48 (shear)	0.62 0.41

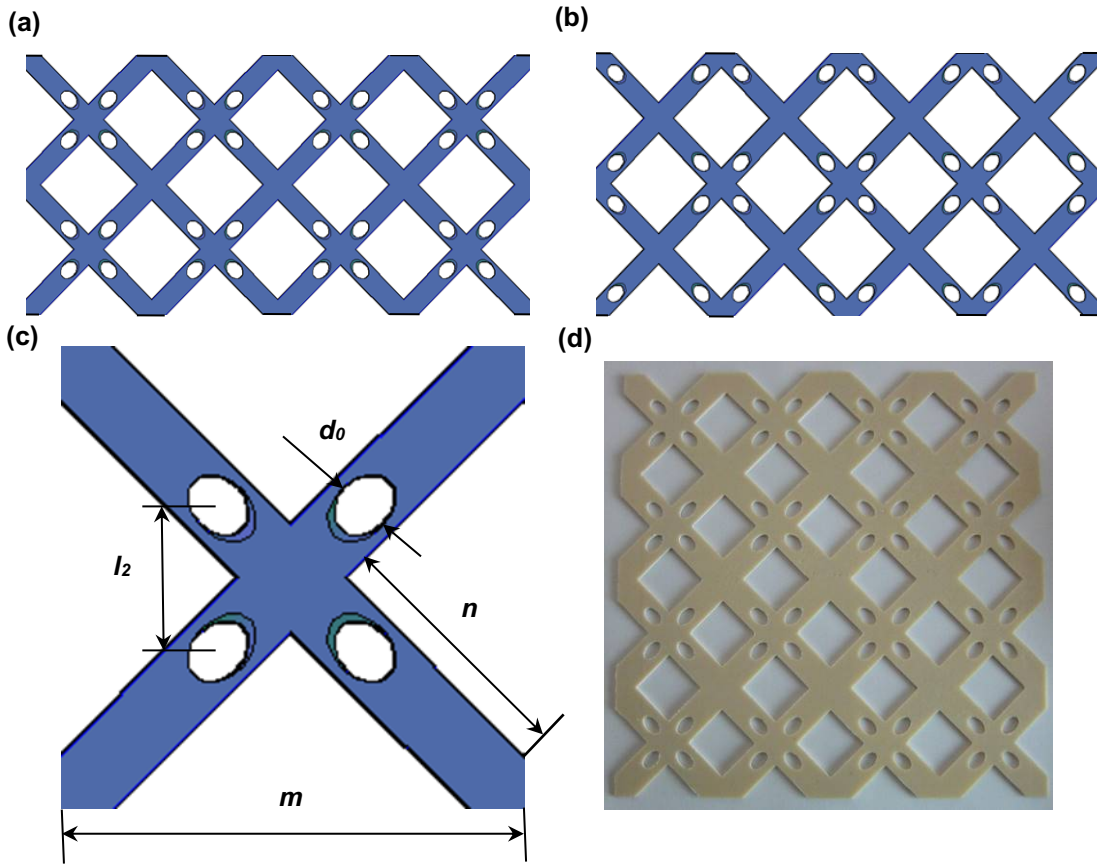

Fig. 1. Patterned 2-D lattice plates with angled holes for guiding truss insertion: (a) upper facesheet; (b) bottom facesheet; (c) representative unit cell of the upper facesheet (d) patterned plate fabricated with glass fiber woven composites.

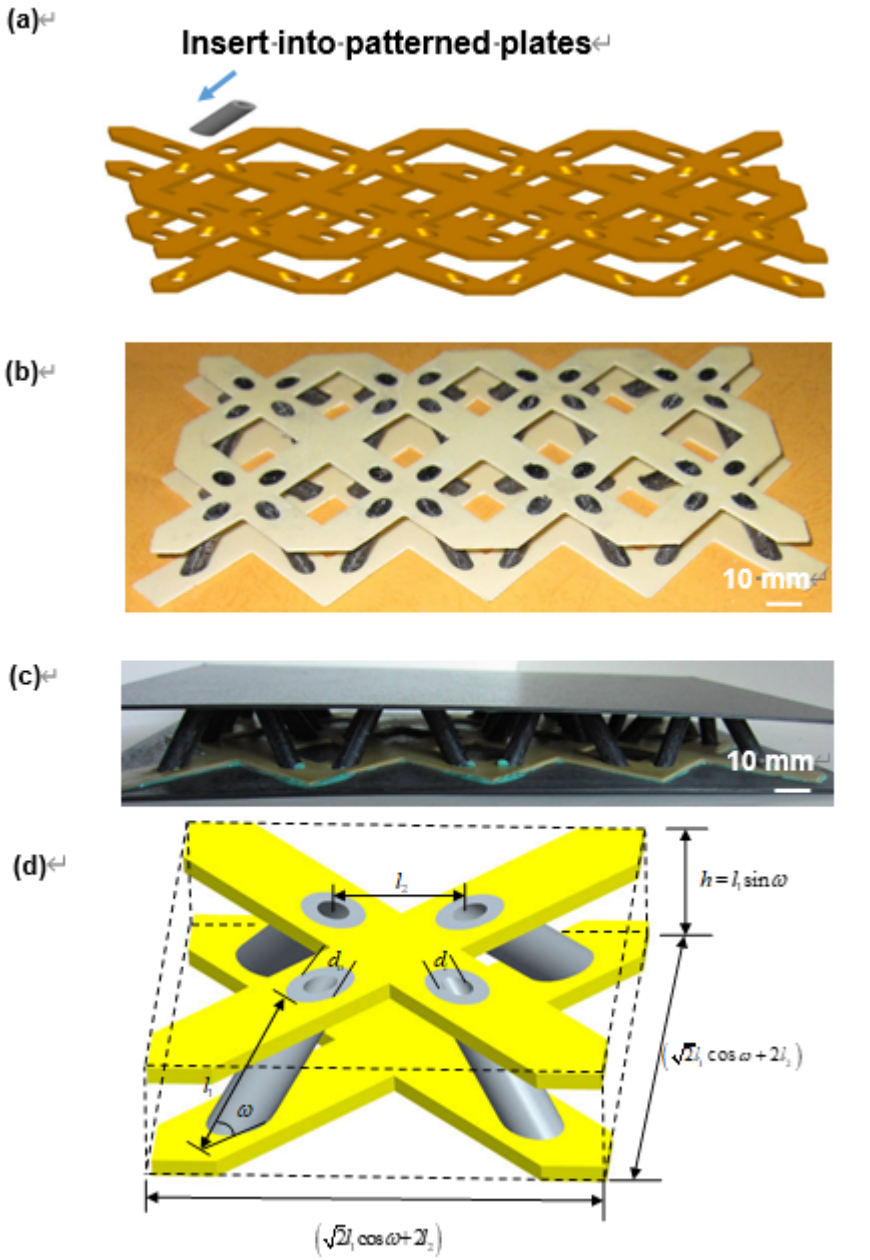

Fig. 2. (a) Illustration of using two patterned plates to guide truss insertion; (b) the assembly of patterned plates and hollow CPL cores; (c) sandwich structure with hollow CPL cores; d) the representative unit cell.

(a)

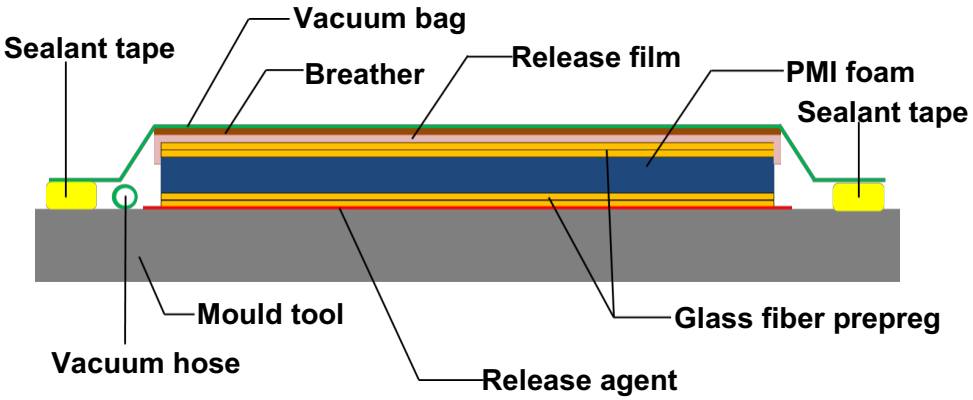
Sealant tape
Vacuum bag
Breather
Release film
PMI foam
Sealant tape
Mould tool
Vacuum hose
Release agent
Glass fiber prepreg

(b)

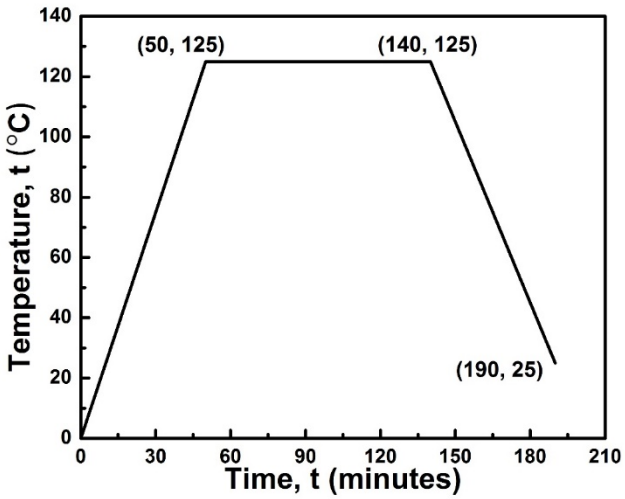
(50, 125)
(140, 125)
(190, 25)
Temperature, t (°C)
Time, t (minutes)
0
20
40
60
80
100
120
140
0
30
60
90
120
150
180
210

(c)

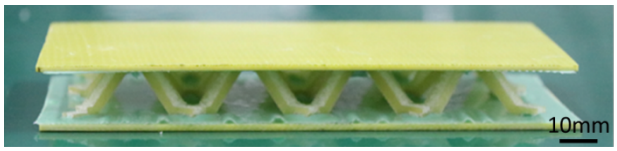
10mm

(d)

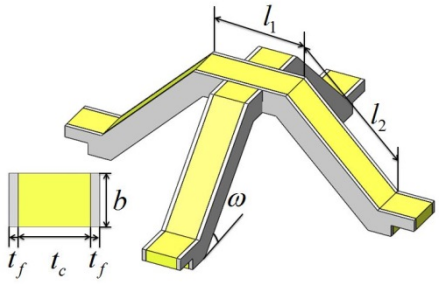
l_1
l_2
b
ω
t_f
t_c
t_f

Fig. 3. a) Vacuum bag only process for the fabrication of foam sandwich panels; b) composites cure cycle; c) the obtained composite lattice cores with foam sandwich trusses; d) the representative unit cell.

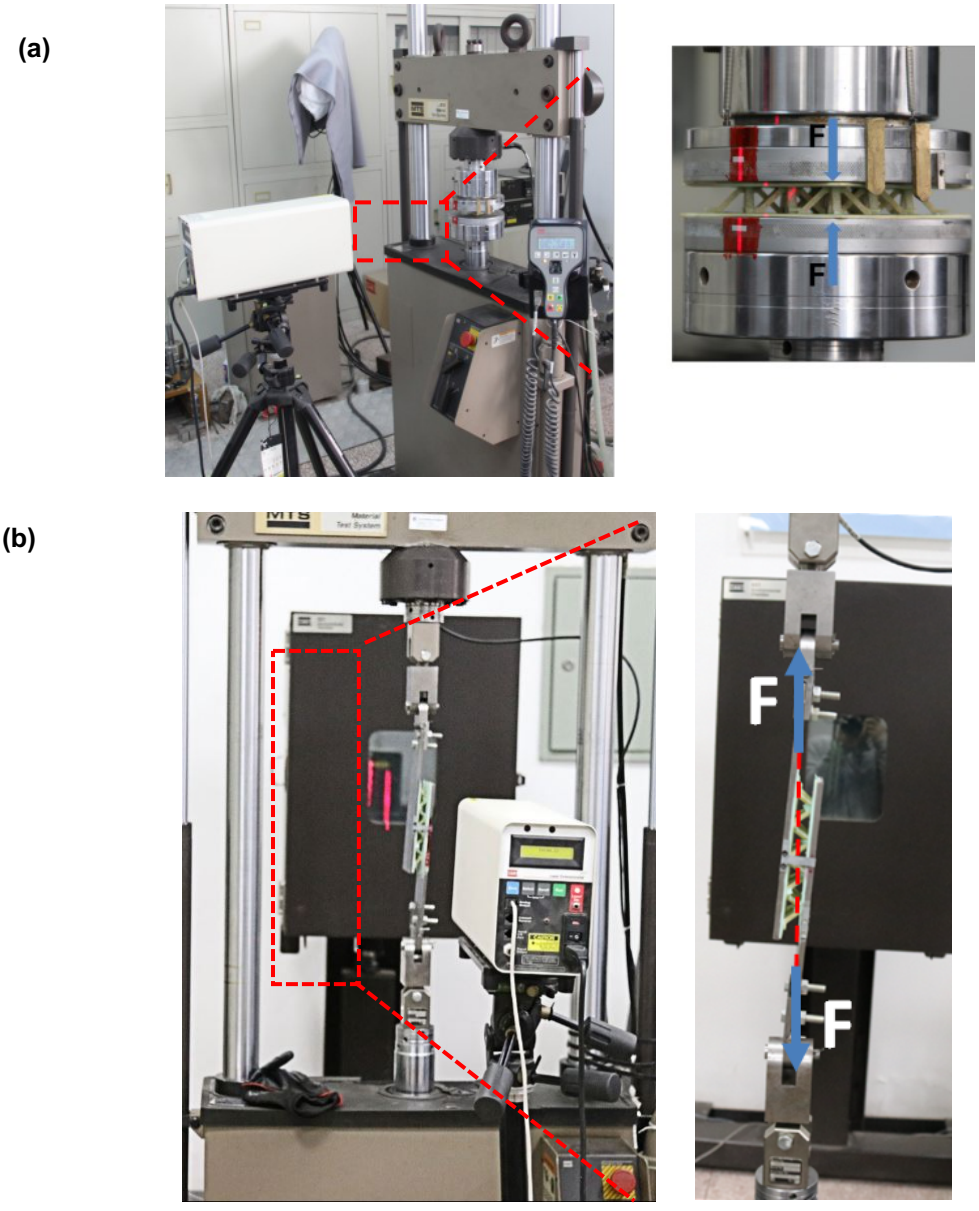

Fig. 4. (a) Lattice truss core sandwich structures in compression; (b) sandwich structure with pyramidal cores loaded in tension, and pure shear was assumed to happen through the lattice core.

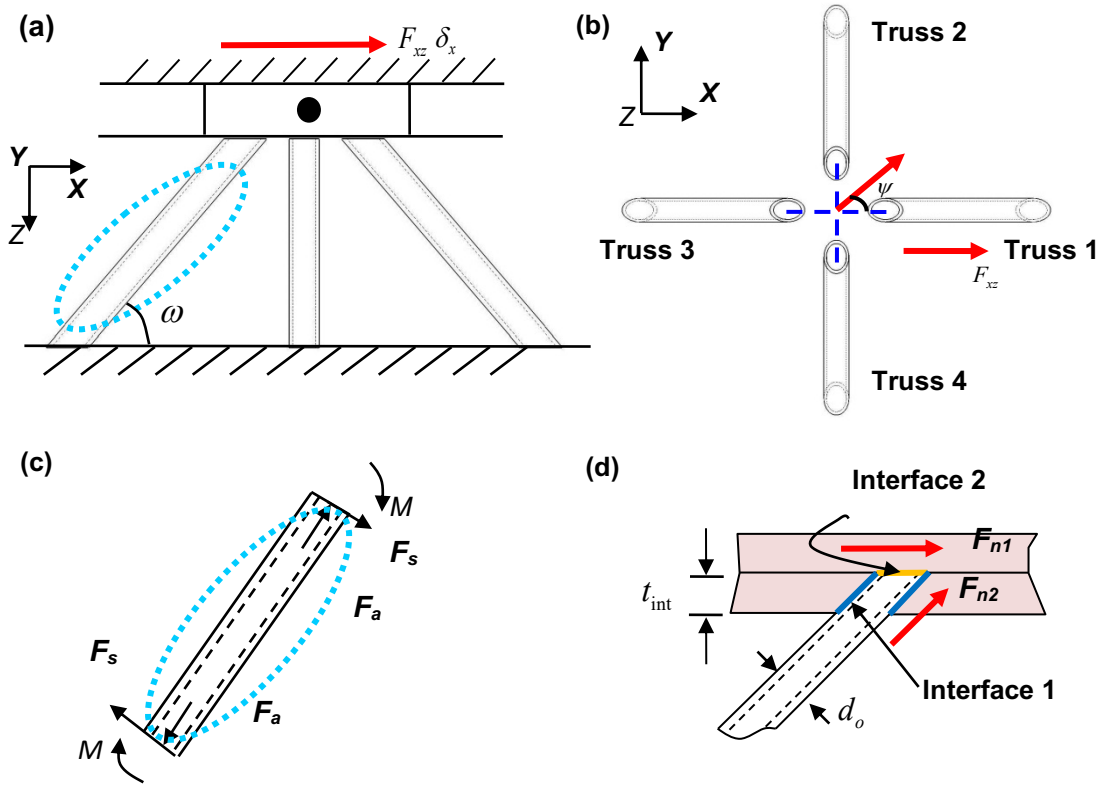

Fig. 5. Theoretical analysis: (a) A representative unit cell of hollow CPL cores in transverse shear loading; (b) top view of the unit cell defining the shear strength direction ψ in the x-y plane; (c) the free-body diagram of a single truss; (d) close-up of the truss/patterned plate/facesheet junction.

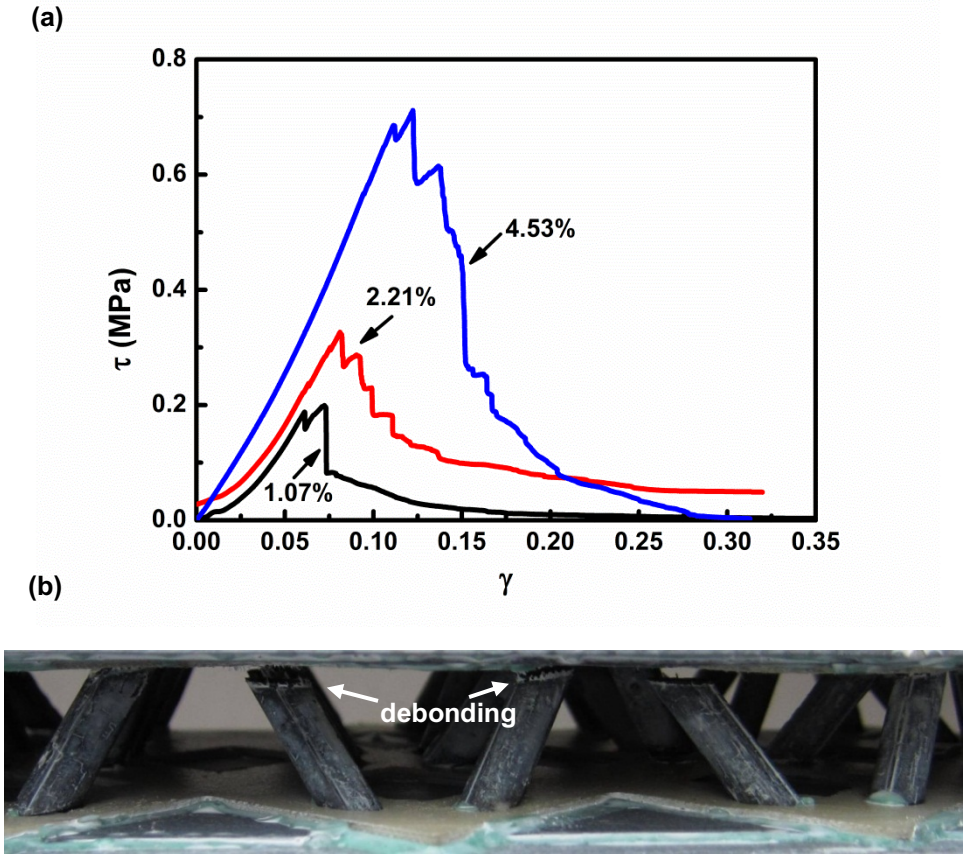

Fig. 6. (a) Shear performance of CPL sandwich structures obtained by the bottom-up assembly technique; (b) the corresponding shear failure modes: debonding between tubes and facesheet was observed for all the samples here.

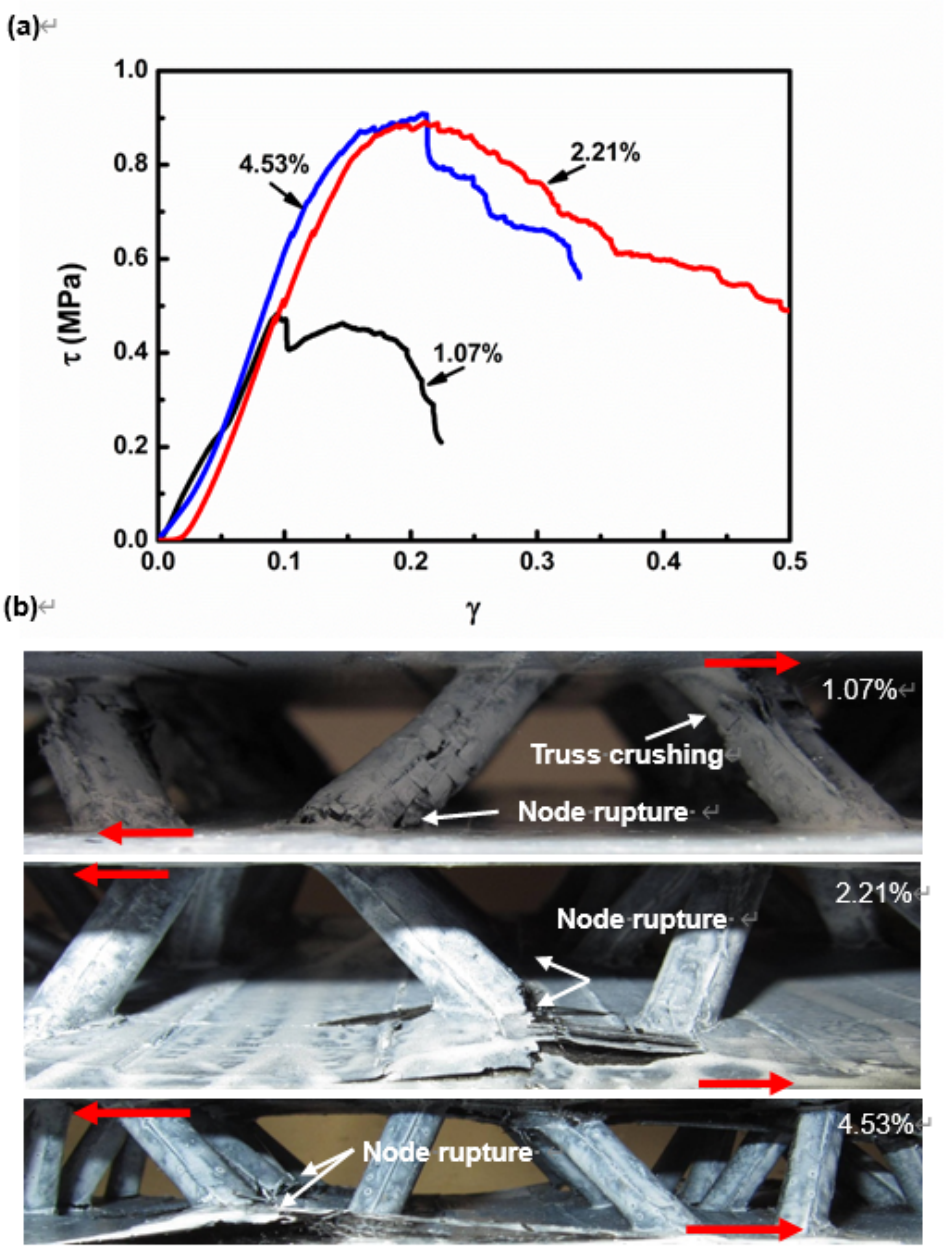

Fig. 7. (a) Shear performance of CPL sandwich structures fabricated with thermal expansion molding technique; (b) the corresponding shear failure modes: node rupture at the tube ends were all observed, while truss crushing happened for the lowest density cores of $\overline{\rho}_h = 1.07\%$.

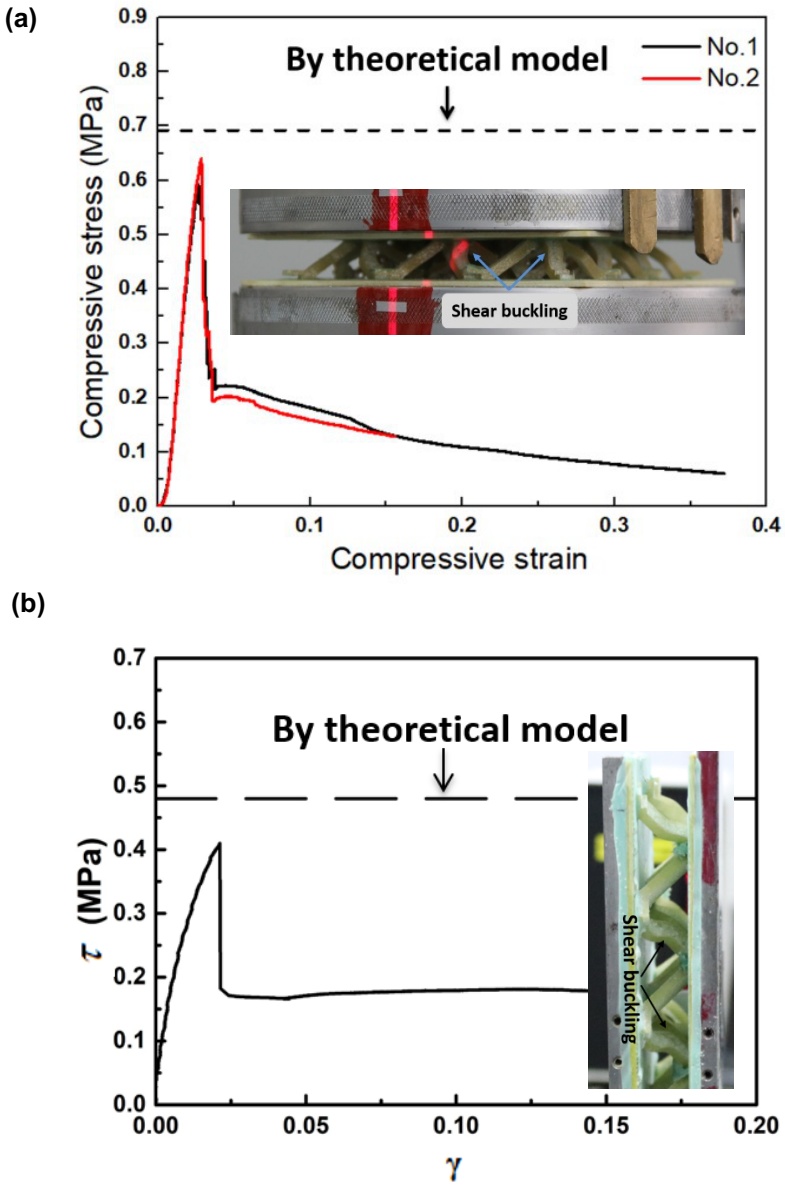

Fig. 8. Overall performance of hierarchical lattice truss core sandwich structures (a) compressive stress-strain curves and the corresponding compression failure mode; (b) shear stress-strain curves and the corresponding shear failure modes.